Journal of Applied Polymer Science

Differences in regenerated silk fibroin prepared with different solvent systems: From structures to conformational changes

Guotao Cheng, Xin Wang, Sijie Tao, Ju Xia, Shui Xu
College of Biotechnology, Southwest University, Beibei, Chongqing 400716, China
Correspondence to: S. Xu (E-mail: xushui1701@163.com)

ABSTRACT: Dissolution is an important part of silk fibroin (SF) reprocessing, and it is the only way to process it into films, gels, porous scaffold materials, and electrostatic spinning silk fibers. There are a variety of dissolution systems used to dissolve SF. However, few studies have focused on the differences between these different solvent systems. The dissolution of SF with different solvent systems was investigated in this study. Regenerated silk fibroin (RSF) solutions and films were characterized by dynamic light scattering, Fourier transform infrared spectroscopy, differential scanning calorimetry, X-ray diffraction, and scanning electron microscopy. The results show that the RSF film structures changed with the solvent system, especially LiBr–H_2O. The characterization proved that the random coil did not change into a β-sheet structure during film formation, and this indicated that its crystal structure and thermal stability was different from others. Interestingly, the differences in the morphologies of all of the RSF films prepared with different solvents were outstanding. Because the mechanism and force of the ion in the solvent systems were different, the SF molecule was hydrolyzed differently in individual solvent systems and produced different hydrolyzed SF molecular chains. These chains had different self-assembly processes and would lead to RSF products with different microstructures and properties. This suggests that a suitable solvent should be chosen for different uses. © 2015 Wiley Periodicals, Inc. J. Appl. Polym. Sci. **2015**, *132*, 41959.

KEYWORDS: biomaterials; films; properties and characterization

Received 9 October 2014; accepted 5 January 2015
DOI: 10.1002/app.41959

INTRODUCTION

Silk has been used as a textile material for a long time because of its beautiful luster and brilliant mechanical properties. SF, one of the most important components of silk, does not irritate or produce an allergic response, it biodegrades, and it has good adhesion and proliferation rates for cells because of its better biocompatibility, safety, and biodegradation properties. It also easy to process into films, sponges, nonwoven fabrics, and gels.[1,2] Thus, SF has been used in food additives and cosmetics and in the biomedical materials field. Silk scaffolds have been successfully used in the tissue engineering of nerve, skin, bone, blood vessel, tendon, ligament, and cornea tissue.[2,3]

Natural SF is a linear, water-insoluble polymer protein. It must be dissolved before it is processed into different forms. There have been a variety of dissolution systems used to dissolve SF. The commonly used solvents include aqueous 9.0–9.5*M* lithium bromide,[4] aqueous 50% calcium chloride,[5] calcium nitrate in methanol,[6–8] mixtures of aqueous calcium chloride and ethanol,[9,10] aqueous lithium bromide and ethanol,[4] aqueous lithium thiocyanate,[11] and aqueous sodium thiocyanate.[12] Hexafluoroisopropanol[13] and novel ionic liquid solvents[14,15] have been also used. However, few studies have focused on the differences between these different solvent systems.[4,5,9,16]

The molecular weight of RSF affects its value in use and control difficultly during degumming and dissolving.[11,16] The molecular weight distributions of RSFs prepared with different solvent systems or the same solvent under different conditions are different.[5,9,10,16,17] Previous studies have confirmed that the smaller the molecular weight is, the harder it is to shape the RSFs during spinning and the easier it is to degrade.[18] The structures of RSF films prepared with different solvent systems are also different.[10] The β-sheet structure is a key factor in the excellent mechanical properties of the silk,[8] but the low molecular weight of RSF influences its conformational change from random coils to a β sheet.[10]

In this study, we selected five common solvent systems to dissolve SF: $CaCl_2$–H_2O, LiBr–H_2O, $CaCl_2$–CH_3CH_2OH–H_2O, LiBr–CH_3CH_2OH–H_2O, and $Ca(NO_3)_2{\cdot}4H_2O$–CH_3OH. The RSF solution and the films were characterized by dynamic light scattering (DLS), Fourier transform infrared (FTIR) spectroscopy, differential scanning calorimetry (DSC), X-ray diffraction (XRD), and scanning electron microscopy (SEM). The dissolution capacity and its effect on the structure are reported.

Table I. Five Solvent Systems Chosen for This Study

Solvent	Preparation
$CaCl_2$–H_2O	50% (weight ratio) $CaCl_2$ aqueous solution
LiBr–H_2O	9M LiBr aqueous solution
$CaCl_2$–CH_3CH_2OH–H_2O	Mixture of $CaCl_2$, CH_3CH_2OH, and H_2O with a molar ratio of 1 : 2 : 8
LiBr–CH_3CH_2OH–H_2O	Mixture of LiBr, CH_3CH_2OH, and H_2O with a weight ratio of 45 : 44 : 11
$Ca(NO_3)_2{\cdot}4H_2O$–CH_3OH	Mixture of $Ca(NO_3)_2{\cdot}4H_2O$ and CH_3OH with a weight ratio of 75 : 25

EXPERIMENTAL

Preparation of the RSF Solution

Bombyx mori cocoons were cut into small pieces and boiled in a 0.5% w/w Na_2CO_3 solution (to degumming cycles, 30-min changes) with a bath ratio of 1 : 50. After degumming, the silk fibers were washed with copious amounts of distilled water and air-dried at room temperature to obtain the SF. Analytical-grade reagents were used throughout.

Five solvent systems (Table I) were used in this study. Five grams of dry SF was dissolved in 50 mL of each solvent at 80°C in a water bath with vigorous magnetic stirring. We noted the time at which no silk fiber could be seen by the eye as the complete dissolution time. After complete dissolution, the RSF solutions were dialyzed (dialysis bags with molecular weight cut offs of 3500) against frequent changes of deionized water for at least 3 days at room temperature. Then, the solution was centrifuged (5000 rpm, 30 min) and filtered. The volume (V; mL) was measured with a cylinder, and we determined the concentration (c; g/mL) of the solution by weighing the dried solid after drying 1 mL of fibroin solutions at 60°C. The yield rate (Y; %) of RSF was determined by eq. (1) as given:

$$Y = Vc/5\,\mathrm{g} \times 100 \quad (1)$$

Characterization of the RSF Solution

We determined the molecular weight of RSF with sodium dodecyl sulfate (SDS)–polyacrylamide gel electrophoresis (PAGE) and 8%–15% gradient gel for electrophoresis, according to published procedures.[19] The 5-mg freeze-dried RSF sample was dissolved in ultrapure water and then centrifuged at 8000 rpm for 5 min. Then, 20 μL of the supernatant was mixed with an equivalent amount of loading buffer (containing 10% SDS, 1% mercaptoethanol, and 8M urea), boiled for 10 min, and then centrifuged at 8000 rpm for 1 min. Then, 10 μL of supernatant was used as the sample. The gel was stained with Coomassie brilliant blue G250.

The self-assembly behavior of the RSF protein in solutions was analyzed by DLS. A dilute RSF solution with a concentration below 0.2% was made from the lyophilized material. This was centrifuged at 15,000 rpm for 15 min, and the supernatant was analyzed by a DLS instrument (BI-200SM, Brookhaven).

RSF Film Preparation

The RSF solution was concentrated, and the film was prepared according to published procedures.[20–23] The dialyzed RSF solution (3–4% w/w) was concentrated at 45°C with slow and constant stirring (50–60 rpm) to 10% w/w for 24 h. Then, the concentrated RSF solution was centrifuged (5000 rpm, 30 min) and filtered. Samples of the 10-mL solution were poured into polystyrene dishes 30 mm in diameter and then dried into films under controlled film-formation conditions (20 ± 5°C, relative humidity = 60%) for 3 days.

RSF Film Characterization

The microstructures of the film samples (sputter-coated with platinum) were observed by SEM (S-4800, Shimadzu, Japan) at an accelerating voltage of 5000 V, working distance of 9800 um, and emission current of 14,800 nA. The RSF films were ground into powders and prepared as KBr pellets suitable for FTIR spectrometry (Spectrum BX, PerkinElmer). For each measurement, 64 scans were collected with a resolution of 4 cm^{-1} and wave numbers from 400 to 4000 cm^{-1}.

The XRD curves were measured by an X-ray diffractometer (XD-3, P General, China) with a diffractometer operating at 36 kV and 20 mA with a Cu Kα target. The RSF powder samples (particle size < 40 μm) were run at diffraction angles (2θs) from 2 to 50° with a step size of 0.01° (2θ) and a scanning rate of 4°/min.

DSC measurements were performed with a differential thermal analysis instrument (STA409, Netzsch, Germany). Five milligrams of the RSF sample was heated to 350°C with a step increase of 10°C/min under an inert argon atmosphere. All of the original data and spectra were analyzed with Origin 8.0 software.

Influence of Ca^{2+} and Ethanol on the Structure of the RSF Films

We divided the RSF solution dissolved in a 9.0M LiBr aqueous solution into five groups at 10 mL per group. To the first, we added nothing; the second received 10 μL of 0.1 g/mL $CaCl_2$, and the third received 50 μL of the same. The fourth received 10 μL of absolute ethanol, and the fifth received 50 μL of the same. We cast the solutions into films and characterized them with SEM and FTIR spectroscopy.

RESULTS AND DISCUSSION

Solubility and Yield Rate of Different Solvent Systems

The dissolving ability of the different solvent systems was judged by the time needed to completely dissolve equal amounts of SF. The SF dissolved easily in all solvents besides $CaCl_2$–H_2O. The other four systems dissolved quickly, almost as soon as the SF was placed in the solvent. In contrast, the $CaCl_2$–H_2O dissolved SF quite slowly; it took at least 6 h at 80°C (Table II). So, the dissolving ability of the solvents could be summarized as follows: $CaCl_2$–H_2O < $CaCl_2$–CH_3CH_2OH–H_2O, $Ca(NO_3)_2{\cdot}4H_2O$–CH_3OH < LiBr–H_2O, LiBr–CH_3CH_2OH–H_2O, as judged from the dissolved time (in minutes).

The yield rates of RSF prepared with different solvent systems were different. In the five solvents, LiBr–H_2O, $CaCl_2$–CH_3CH_2OH–H_2O, and LiBr–CH_3CH_2OH–H_2O were very close,

Table II. Times for the Complete Dissolution and Yield Rate of RSF Prepared with Different Solvent Systems

Solvent	Dissolved time (min)	Yield rate (%)[a]
$CaCl_2$-H_2O	360	59.0 ± 5.3
LiBr-H_2O	4-5	94.3 ± 4.2
$CaCl_2$-CH_3CH_2OH-H_2O	10-15	93.6 ± 2.5
LiBr-CH_3CH_2OH-H_2O	4-5	92.7 ± 2.1
$Ca(NO_3)_2{\cdot}4H_2O$-CH_3OH	25-30	76.6 ± 0.9

[a] Mean ± standard deviation.

with yield rates surpassing 90%. The $CaCl_2$–H_2O and $Ca(NO_3)_2{\cdot}4H_2O$–CH_3OH had low yield rates (Table II). This may have been because these two solutions were too thick with a poor transfer to the dialysis bags. In addition, a small amount of insoluble substance was subsided during dialysis of the fibroin solution prepared with $CaCl_2$–H_2O, although no filamentous silk fiber was seen by the eye after 6 h of dissolution.

Molecular Weight Distribution of the RSF Solutions

The molecular weight of RSF is a problem and has puzzled researchers for a long time. We used SDS–PAGE to study it here. There were two broad smeared bands at 100 and 25 kDa for all of the samples (Figure 1, lanes 1–4) except sample 5 (Figure 1, lane 5). Yamada *et al.*[11] used SDS–PAGE to analyze the native fibroin, and the result revealed clear protein bands having molecular weights of about 350 and 25 kDa, which corresponded to the H and L chains of the SF. Our SDS–PAGE result indicated that the native fibroin molecule (H chain) was degraded to a mixture of polypeptides of various sizes during the dissolution processes, and it showed a broad, smeared band around 100 kDa. The solvents $CaCl_2$–H_2O, LiBr–H_2O, $CaCl_2$–CH_3CH_2OH–H_2O, and LiBr–CH_3CH_2OH–H_2O seemed to have

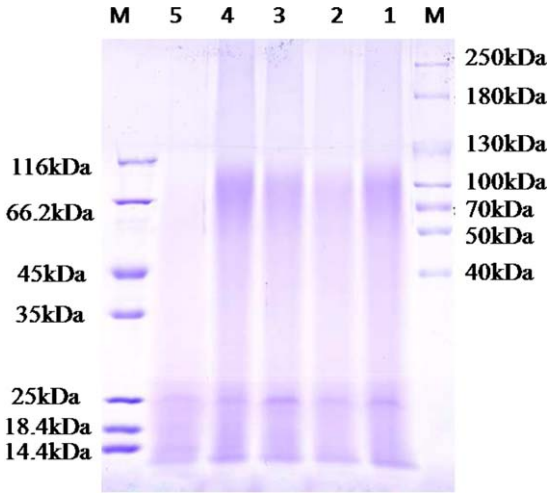

Figure 1. SDS–PAGE results for SF prepared with different solvent systems: (1) $CaCl_2$–H_2O, (2) LiBr–H_2O, (3) $CaCl_2$–CH_3CH_2OH–H_2O, (4) LiBr–CH_3CH_2OH–H_2O, and (5) $Ca(NO_3)_2{\cdot}4H_2O$–CH_3OH. M indicates a marker. [Color figure can be viewed in the online issue, which is available at wileyonlinelibrary.com.]

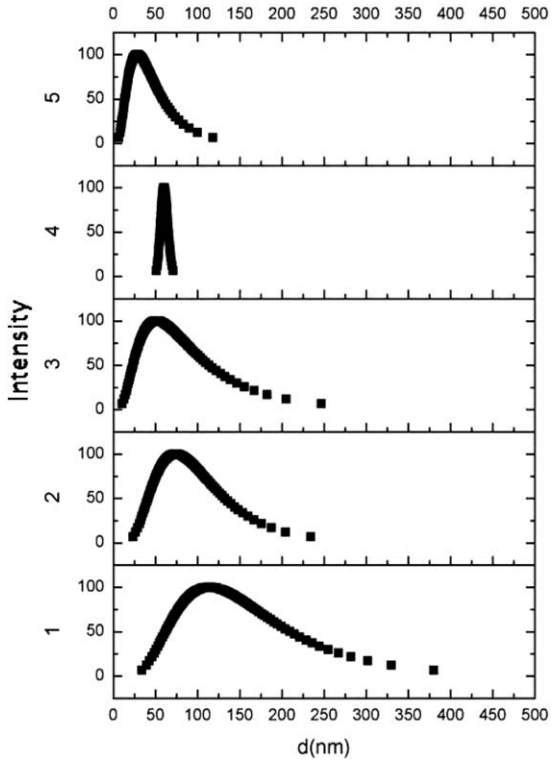

Figure 2. Particle size distributions of the RSF solutions dissolved with different solvent systems: (1) CaCl2–H2O, (2) LiBr–H2O, (3) CaCl2–CH3CH2OH–H2O, (4) LiBr–CH3CH2OH–H2O, and (5) Ca(NO3)2·4H2O–CH3OH. d = diameter.

a similar degradation and molecular weight distribution. However, the solvent $Ca(NO_3)_2{\cdot}4H_2O$–CH_3OH degraded more. The molecular weight of RSF was affected by various factors during the solution-preparing process.[11] Not only did the different solvents have different abilities to degrade SF with different molecular weights but also the same solvent under different conditions.[16,17] Wang[16] reported that the degradation degree of the SF molecular chains in LiBr–H_2O was less than that in $CaCl_2$–CH_3CH_2OH–H_2O. This did not conflict with our result because of the different dissolution conditions.

Self-Assembly of the Different RSF Solutions

Jin and Kaplan[24] put forward the model of chain folding and micelle formation of the silk fibroin (SF) chain. The SF chain is a long hydrophilic–hydrophobic–hydrophilic polymer and will fold into a 20-nm micelle with hydrophobic and hydrophilic interactions in aqueous solutions. The DLS analysis of the five RSF solutions prepared with different solvent systems showed different self-assembly results (Figure 2) of the five RSF solutions, even though they had similar molecular weight distributions. The micelles of RSF from the $CaCl_2$–H_2O solvent had the widest size distribution, which ranged from 20 to 400 nm (average size = 128.8 ± 66.6 nm), compared to the most homogeneous size distribution of 50–75 nm (average size = 60.5 ± 4.1 nm) for the LiBr–CH_3CH_2OH–H_2O solvent. The RSF solution in $Ca(NO_3)_2{\cdot}4H_2O$–CH_3OH showed a small average particle size of 33.89 ± 20.9 nm because the SF molecular chains degraded more in the solvent solutions. The

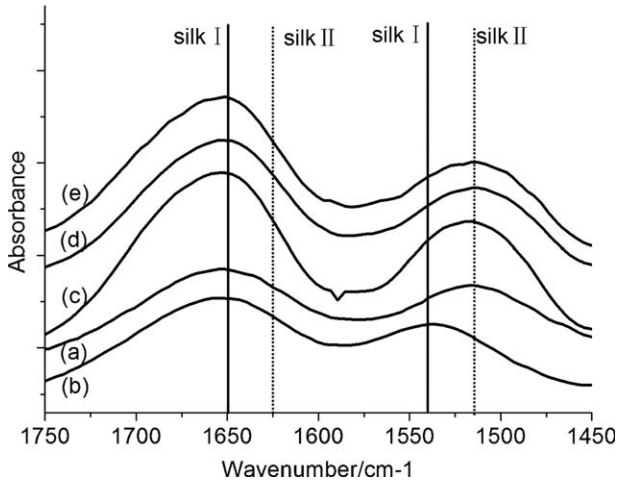

Figure 3. FTIR spectra of the RSF films prepared with different solvent systems: (a) CaCl2–H2O, (b) LiBr–H2O, (c) CaCl2–CH3CH2OH–H2O, (d) LiBr–CH3CH2OH–H2O, and (e) Ca(NO3)2·4H2O–CH3OH.

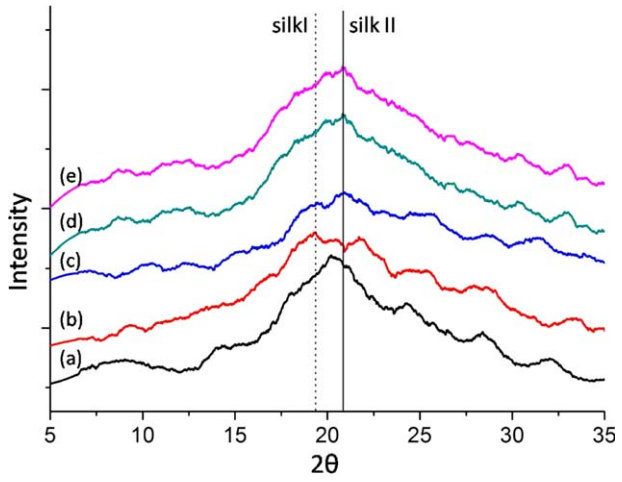

Figure 4. XRD results for the RSF films prepared with different solvent systems: (a) CaCl2–H2O, (b) LiBr–H2O, (c) CaCl2–CH3CH2OH–H2O, (d) LiBr–CH3CH2OH–H2O, and (e) Ca(NO3)2·4H2O–CH3OH. [Color figure can be viewed in the online issue, which is available at wileyonlinelibrary.com.]

$LiBr–H_2O$ and $CaCl_2–CH_3CH_2OH–H_2O$ showed similar average particle sizes of 82.7 ± 40.8 and 63.2 ± 43.5 nm, respectively.

Cho *et al.*[17] reported that when the regenerated silk fibroin (RSF) chain was integrating after dissolution, it had a size range of 10–30 nm compared to 100–300 nm when the chain was hydrolyzed. In our study, the micelle size of the RSF protein was larger than 30 nm; this suggested that all of the RSF protein was hydrolyzed during dissolution. This was also verified by SDS–PAGE. SDS–PAGE analysis showed that the RSF solutions from different solvent systems had similar molecular weight distributions and, thus, formed micelles with similar size distributions. However, the micelles of the five RSF were different in size; this meant that SF was hydrolyzed differently in different solvent systems during dissolution.

Inorganic salt generates ions in water and increases the polarity of the water molecules. This undermines the intermolecular forces of SF and swells the silk.[25] Alcohol can enter the crystalline regions of SF and make the hydrophobic crystalline regions more hydrophilic; this promotes the dissolution of SF.[7,26] However, different ions have different effects on SF peptide bonds and amino acids. For example, calcium ions (Ca^{2+}) in calcium salt solvent can form hydrated Ca^{2+}, and the presence of ethanol (ROH) increases its permeability. The hydrated Ca^{2+} can form a stable chelate complex with the hydroxyl group of the side chains of serine and tyrosine of SF molecules and remove hydrogen bonds and van der Waal's forces between the polypeptide chains. This disperses the SF molecules independently for complete dissolution.[27] The Br^- has electrophilic substitution reactions with the phenolic hydroxyl groups of tyrosine of SF.[27] Ha *et al.*[7] also believed that the dissolution of SF depends not only on Ca^{2+} and its ligand oxygen atoms but also on nitrate ions (NO_3^-). Thus, we attributed the SF dissolution features in various solvents to the differences in the key ions (Br^-, Ca^{2+}) and counter ions (Cl^-, NO_3^-) and to the water–alcohol types and proportions present in these different solvents. Different solvents produced different hydrolyzed SF molecular chains and led to different self-assemblies of RSF.

Structure of the RSF Film and Conformation Transition in the Film-Forming Process

Silk I and silk II are two kinds of SF molecular structures, and they are frequently used to analyze the SF structure. Silk I (the black solid line in Figure 3) is composed of random coils and an α-helix, which shows an amide I bond at 1650 $cm^{-1}$and an amide II bond at 1545 cm^{-1}. Silk II (the black dotted line in Figure 3) mainly is β sheets, which show an amide I bond at 1625 $cm^{-1}$and an amide II bond at 1515 cm^{-1}.[22,28,29] The SF chains were random coils in the dilute solution, but the conformation changed to an α helix and further to a β sheet during film formation.[28,29] The structure of the RSF films was analyzed by FTIR spectroscopy (Figure 3). The spectra showed that the amide I bonds of all of RSF films appeared at 1650 cm^{-1} and indicated random coil and α-helix structures (silk I). The amide

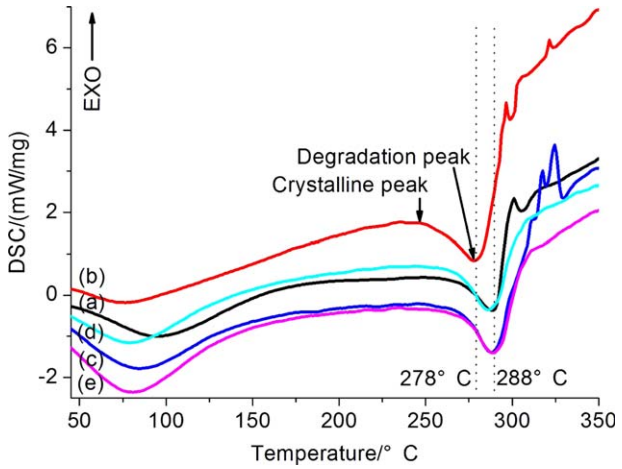

Figure 5. DSC curves of the RSF films prepared with different solvent systems: (a) CaCl2–H2O, (b) LiBr–H2O, (c) CaCl2–CH3CH2OH–H2O, (d) LiBr–CH3CH2OH–H2O, and (e) Ca(NO3)2·4H2O–CH3OH. [Color figure can be viewed in the online issue, which is available at wileyonlinelibrary.com.]

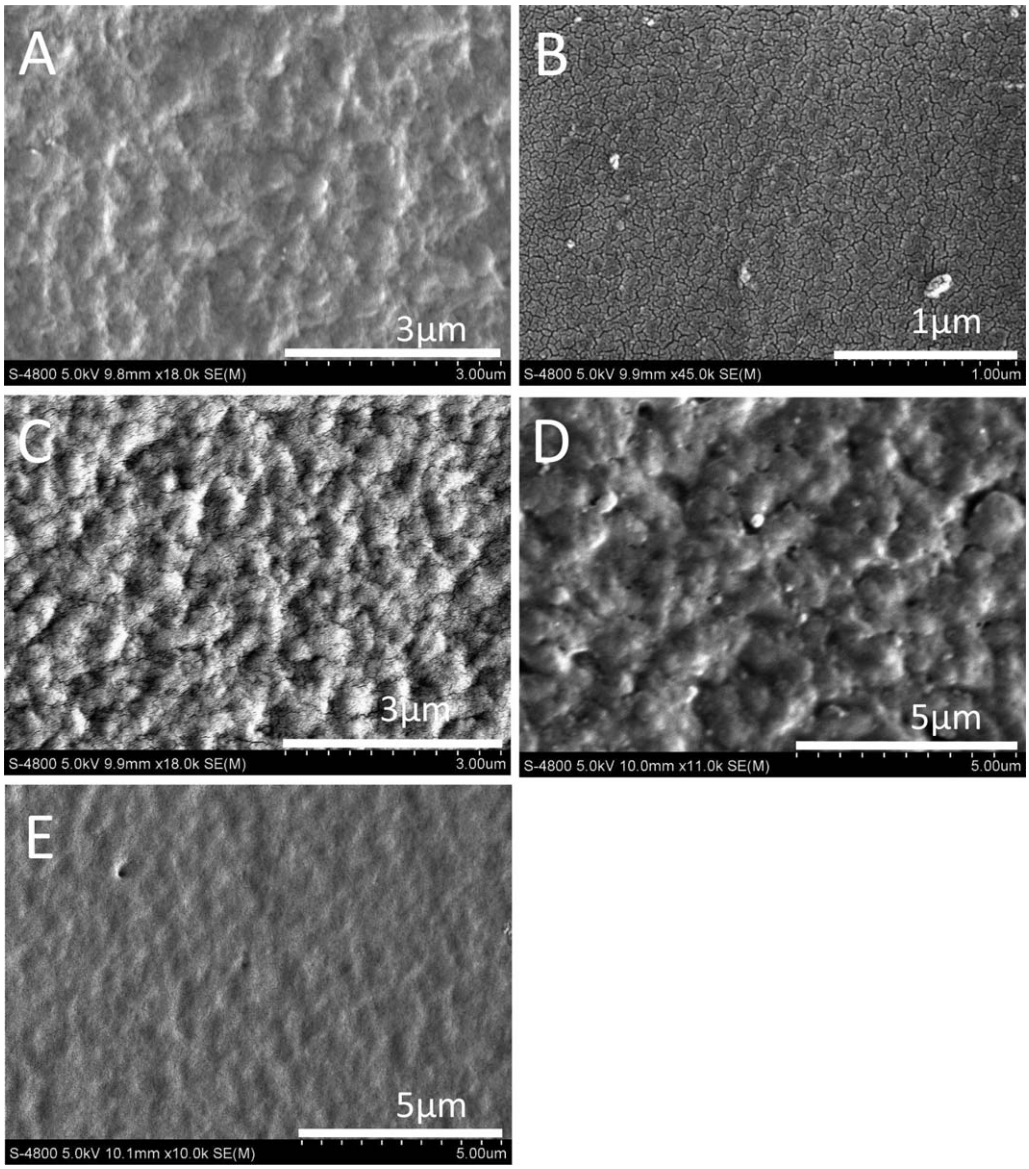

Figure 6. SEM photos of the RSF films prepared with different solvent systems: (A) CaCl2–H2O, (B) LiBr–H2O, (C) CaCl2–CH3CH2OH–H2O, (D) LiBr–CH3CH2OH–H2O, and (E) Ca(NO3)2·4H2O–CH3OH.

II bonds appeared at 1515 cm^{-1} and indicated β-sheet structures (silk II). However, the amide II bond of the LiBr–H_2O sample appeared at 1540 cm^{-1}; this indicated that its structure was an α helix (silk I). The results show that the β-sheet structures appeared in all of the RSF films except the LiBr–H_2O sample. This corresponded to previous work.[4,5,10]

The secondary structure of the RSF film was further characterized by XRD. The XRD results (Figure 4) indicate that all of the RSF films had relatively strong diffraction peaks around a 2θ of 20°. However, the LiBr–H_2O sample showed two weak peaks around 20°. Ha and coworkers[7,8] reported that natural silk fibers have strong diffraction peaks at a 2θ of 21°, but the peak intensity decreases, and the crystallinity reduces after dissolution and regeneration. From the analysis of the crystal type (silk I and silk II), the films all existed with a silk II structure ($2\theta = 20.7°$, the black solid line in Figure 4), but the film from LiBr–H_2O was silk I ($2\theta = 19.7°$, the black dotted line in Figure 4).[30] This was consistent with the FTIR results.

The structural differences were also confirmed by DSC (Figure 5). The trends of the DSC curves were basically the same, and the degradation peak was near 280°C, whereas the thermal degradation temperature of the film from LiBr–H_2O was 278°C. This was lower than that of the other four (288°C). Furthermore, there was a weak crystalline peak at 250°C in the DSC curve of the LiBr–H_2O sample; this indicated that some unstable amorphous structures had changed into a stable β sheet here.[22] The crystalline peak of the other four disappeared indicated that they formed before the measurements. This was consistent with the previous results of FTIR spectroscopy and XRD. Except for the LiBr–H_2O sample, the other four had an

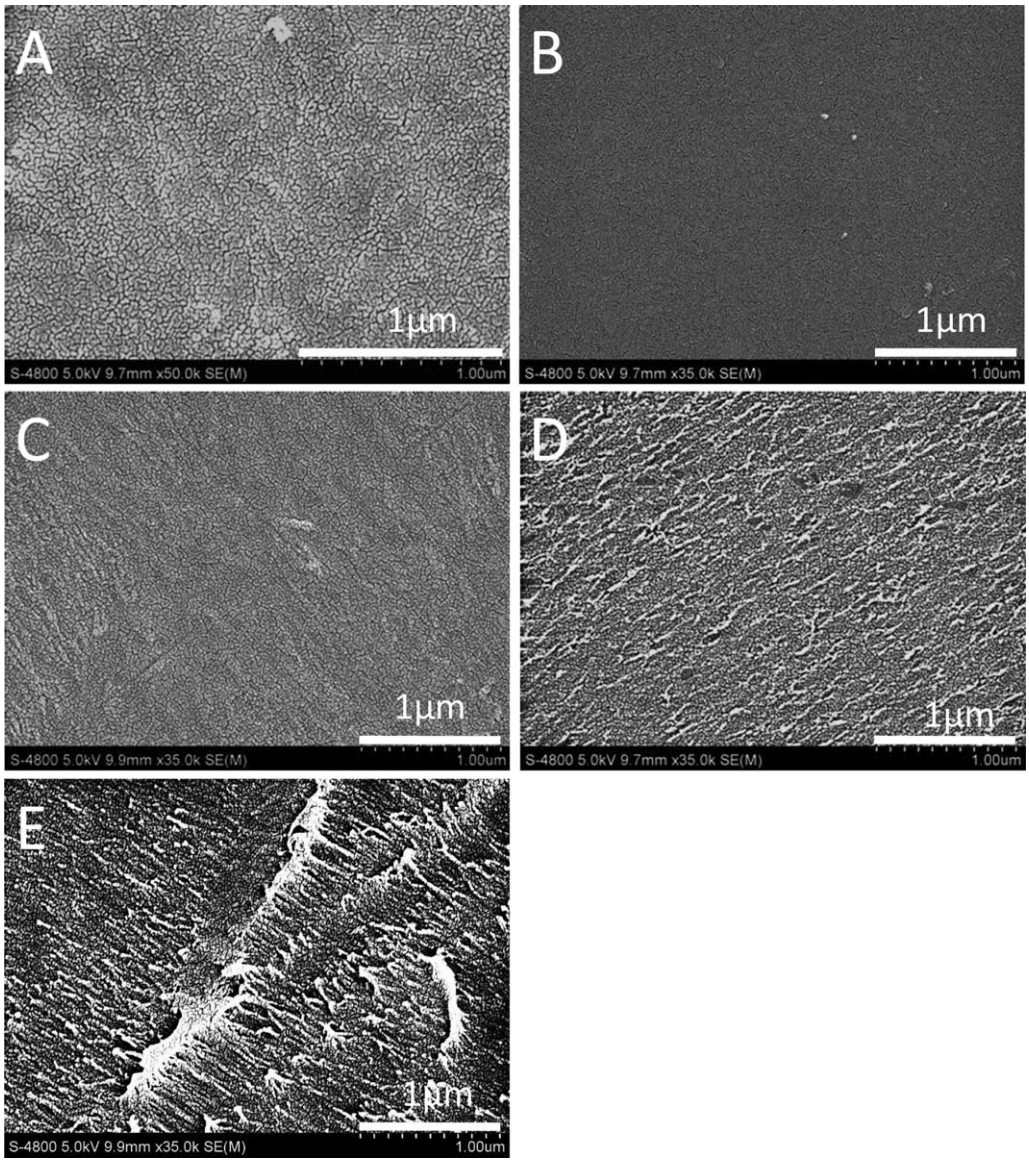

Figure 7. SEM photos of the RSF films with Ca2+ and alcohol added: (A) RSF film dissolved with LiBr–H2O, (B) film A with 10 μL of Ca2+ (the Ca2+ concentration was about 100 ppm, that is, equal to the residual quantity of the SF solution after dialysis), (C) film A with 50 μL of Ca2+, (D) film A with 10 μL of ethanol, and (E) film A with 50 μL of ethanol.

increased β-sheet content and formed silk II crystal structures already. The structural difference led to the degradation temperature of the LiBr–H_2O sample (278°C) being lower than that of the others (288°C) because the silk I crystal structure had less thermal stability than silk II.[22]

The SF film is an important carrier for studying the conformational transition of SF. Magoshi[31] went deep into the crystal morphology of the SF solution solidified at different concentrations and temperatures. A variety of substances and ions could induce SF molecular chains into β sheets; these included methanol, ethanol, formic acid, chitosan, Cu^{2+}, and Ca^{2+}.[28,32–35] Furthermore, the temperature, humidity, pH, air, ultrasound, polyhydric alcohols, and shear force also accelerated the SF changes from silk I to silk II.[21–23,30,36] The native fibroin molecule degraded during the dissolution process. Previous research[5,10] indicated that a higher degree of degradation and a smaller molecular weight made RSF more difficult to form α-helix and β-sheet structures during film formation. In our study, we found that the RSF from LiBr–H_2O was difficult in conformational transition, but it had a similar molecular weight to the others. Furthermore, the RSF from $Ca(NO_3)_2{\cdot}4H_2O$–CH_3OH had the smallest molecular weight, but it did not have difficulty in conformational change. Chen *et al.*[37] reported that the β-sheet structure that formed initially was particularly important to its follow-up transition from disorder to regular during the conformational transition of the SF film. Thus, we surmised that the size of the RSF molecular weight was not intimately linked with its conformational transition.

Surface Morphology of the RSF

The morphology of the RSF sample was investigated by SEM. The surface microstructures of the five films were completely different (Figure 6). The small cracks on the film were due to the contraction of the samples during drying. All of the films formed irregular globulelike structures of different sizes on their surface except samples B and E. The globulelike structure of samples A and C were smaller (200–500 nm) but larger in density. Sample D had bigger globules (ca. 500 nm) but a lower density. Sample E had no significant globulelike structures and showed an uneven surface. Those globulelike structures might have contributed to the film-forming method of RSF. Lv *et al.*[22] reported that a globulelike structure formed when the RSF film was prepared with very slow drying. The SF molecules were in solution for a long time; this gave them a higher molecular mobility and a larger space to self-assemble, and thus, globules were formed because the nanofilaments were entangled.[22] The structure was composed of silk I and silk II, surrounded by hydrophilic nanofilaments, which contained random turns and α-helix structures. The globule structure was different in size, and this indicated that the RSFs prepared with different solvent systems were different and had different self-assembly processes. This led to differences in the film morphology. Generally, the film prepared with LiBr–H_2O did not show that the globulelike structure on the film surface might have contributed to the conformational change from α helix to β sheet.

Influence of Ca^{2+} and Ethanol on the RSF Structure

The previous study reported that there was still a small amount of Ca^{2+} retained in the RSF solution, which was prepared with calcium salt after dialysis,[7] and Ca^{2+} had a big effect on the conformational change of SF.[28] To investigate whether this was the main cause of the differences, we added Ca^{2+} into the SF solution, which was prepared with LiBr–H_2O and cast into films. The Ca^{2+} concentration of the SF solution was about 100 ppm, which was equal to the residual quantity of the Ca^{2+} in SF solution prepared with the calcium salt solvent after dialysis. From the SEM photos [Figure 7(A–C)] of the films, we found that both films, with or without Ca^{2+}, were smooth. The FTIR spectra (Figure 8) of the RSF films with added Ca^{2+} showed that the secondary structure of the RSF did not change either. This indicated that the residual Ca^{2+} after dialysis was not sufficient to cause obvious conformational changes in the RSF films. When we increased the quantity of Ca^{2+} to five times the residual quantity, the wave number of the FTIR characteristic peaks moved from random coil (1655 cm^{-1}) to α helix (1650 cm^{-1}), as shown in Table III.

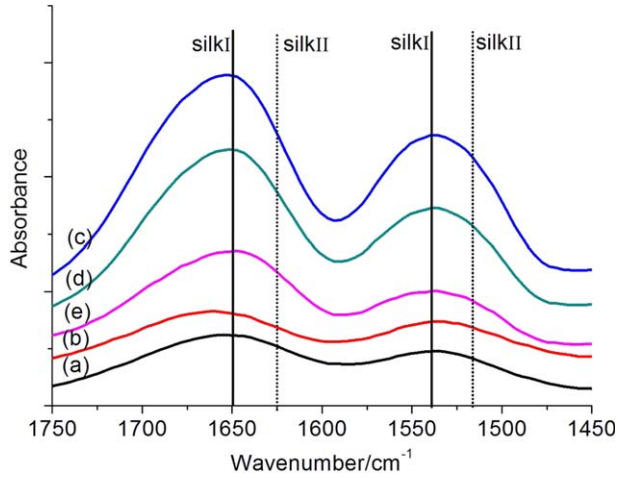

Figure 8. FTIR spectra of the RSF films with Ca2+ and ethanol added: (a) RSF film dissolved with LiBr–H2O, (b) film A with 10 μL of Ca2+, (c) film A with 50 μL of Ca2+, (d) film A with 10 μL of ethanol, and (e) film A with 50 μL of ethanol. [Color figure can be viewed in the online issue, which is available at wileyonlinelibrary.com.]

Table III. FTIR Characteristic Peaks of SF Films with Ca^{2+} and Ethanol Added

Fibroin films	Amide I	Amide II
A. Dissolved with LiBr–H_2O	1654.92	1535.34
B. Film A + 10 μL of Ca^{2+}	1658.78	1535.34
C. Film A + 50 μL of Ca^{2+}	1651.07	1539.20
D. Film A + 10 μL of ethanol	1651.07	1539.20
E. Film A + 50 μL of ethanol	1647.21	1539.20

Hydrophilic alcohols, such as methanol and ethanol, could enter into the SF molecules, change the conformation, and bring small nanofilament structures in the film.[22,32,38] The SEM results showed that the RSF films added with alcohol had a nanofilament structure on their surface [Figure 7(D)] and became more obvious with increasing ethanol content [Figure 7(E)]. The FTIR results also confirmed that the characteristic peaks moved near the α helix (Figure 8 and Table III). The results indicate that the alcohols could affect the structure of RSF, in accordance with a previous study.[22,38] However, the surface structures of the RSF films with ethanol were the nanofilament structure; this was quite different from the globulelike structure observed before (Figure 6). Therefore, we concluded that the residual Ca^{2+} and ethanol were not the main cause of the differences in the RSF films.

CONCLUSIONS

We reported differences in different solvent systems dissolving SF and the effects on the structure and conformational transitions of the RSFs. The different solvent systems had different abilities and yield rates in the dissolution of SF. Because of the mechanism and the force of the ion in the solvent systems were different, the SF was hydrolyzed differently in individual solvent systems during dissolution. This affected the self-assembly of the RSF solution and the structures of the RSF films.

The RSF films made by LiBr–H_2O was quite different from the other four films. The structural characterization indicated that the conformation of RSF did not change from random coil and α helix to β sheet; this imparted a different crystal structure and thermal stability. Interestingly, the difference was much more significant in the morphology of the RSF films. The five films all had special structures.

The previous analysis suggests that we can choose a suitable solvent for different purposes. For example, LiBr–H_2O is best for

studying the conformational transition of SF because LiBr–H_2O would not promote the conformation transition of RSF. LiBr–H_2O is also the best choice when preparing products with excellent optical performance, such as artificial corneas[39,40] and invisible glasses, because of its smooth surface. If there is no special requirement to RSF, we can select $CaCl_2$–CH_3CH_2OH–H_2O because it dissolves SF rapidly with a high yield rate and low cost.

ACKNOWLEDGMENTS

This work was supported by the Fundamental Research Funds for the Central Universities (contract grant number XDJK2012C010).

REFERENCES

1. Vepari, C.; Kaplan, D. *Prog. Polym. Sci.* **2007**, *32*, 991.
2. Unger, R.; Wolf, M.; Peters, K.; Motta, A.; Migliaresi, C.; Kirkpatrick, C. *Biomaterials* **2004**, *25*, 1069.
3. Hardy, J.; Romer, L.; Scheibel, T. *Polymer* **2008**, *49*, 4309.
4. Chen, X.; Knight, D.; Shao, Z.; Vollrath, F. *Polymer* **2001**, *42*, 9969.
5. Liu, M. Studies on the Conformation of Silk Fibroin by FTIR; Zhejiang University: Hangzhou, China, **2006**.
6. Mathur, A.; Tonelli, A.; Rathke, T.; Hudson, S. *Biopolymers* **1997**, *42*, 61.
7. Ha, S.; Park, Y.; Hudson, S. *Biomacromolecules* **2003**, *4*, 488.
8. Ha, S.; Tonelli, A.; Hudson, S. *Biomacromolecules* **2005**, *6*, 1722.
9. Zhang, H.; Li, L.; Dai, F.; Zhang, H.; Ni, B.; Zhou, W.; Yang, X.; Wu, Y. *J. Translat. Med.* **2012**, *10*.
10. Wu, Z.; Feng, X.; Zhu, H.; Liu, N.; Sun, B.; Wu, B.; Chen, J. *Sci. Seric.* **2010**, *36*, 707.
11. Yamada, H.; Nakao, H.; Takasu, Y.; Tsubouchi, K. *Mater. Sci. Eng. C* **2001**, *14*, 41.
12. Sun, Y.; Shao, Z.; Ma, M.; Hu, P.; Liu, Y.; Yu, T. *J. Appl. Polym. Sci.* **1997**, *65*, 959.
13. Zhu, Z.; Ohgo, K.; Asakura, T. *Express Polym. Lett.* **2008**, *2*, 885.
14. Goujon, N.; Wang, X. G.; Rajkowa, R.; Byrne, N. *Chem. Commun.* **2012**, *48*, 1278.
15. Wang, Q.; Yang, Y.; Chen, X.; Shao, Z. *Biomacromolecules* **2012**, *13*, 1875.
16. Wang, Q.; Chen, Q.; Yang, Y.; Shao, Z. *Biomacromolecules* **2013**, *14*, 285.
17. Cho, H.; Ki, C.; Oh, H.; Lee, K.; Um, I. *Int. J. Biol. Macromol.* **2012**, *51*, 336.
18. Cho, H.; Yoo, Y.; Kim, J.; Park, Y.; Bae, D.; Um, I. *Polym. Degrad. Stab.* **2012**, *97*, 1060.
19. Yu, T.; Cai, Z.; Huang, W. *Chem. J. Chin. Univ. Chin.* **1996**, *17*, 829.
20. Lv, Q.; Cao, C.; Zhai, H.; Zhu, H. *Chin. Sci. Bull.* **2004**, *47*, 538.
21. Min, S.; Kai, T.; Teramoto, A.; Abe, K. *J. Seric. Sci. Jpn.* **1997**, *66*, 387.
22. Lv, Q.; Hu, X.; Wang, X.; Kluge, J.; Lu, S.; Cebe, P.; Kaplan, D. *Acta Biomater.* **2010**, *6*, 1380.
23. Zhang, C.; Song, D.; Lv, Q.; Hu, X.; Kaplan, D.; Zhu, H. *Biomacromolecules* **2012**, *13*, 2148.
24. Jin, H.; Kaplan, D. *Nature* **2003**, *424*, 1057.
25. Ni, L.; Wang, Z.; Yao, W.; Xu, S. *J. Chin. Inst. Food Sci. Technol.* **2001**, *1*, 12.
26. Hino, T.; Tanimoto, M.; Shimabayashi, S. *J. Colloid Interface Sci.* **2003**, *266*, 68.
27. Mei, S.; Shao, X.; Liu, W.; Chen, J.; Liu, D. *J. Suzhou Inst. Silk Text. Technol.* **1983**, *1*, 63.
28. Li, G.; Zhou, P.; Shao, Z.; Xie, X.; Chen, X.; Wang, H.; Chunyu, L.; Yu, T. *Eur. J. Biochem.* **2001**, *268*, 6600.
29. Chen, X.; Shao, Z.; Knight, D.; Vollrath, F. *Proteins Struct. Funct. Bioinf.* **2007**, *68*, 223.
30. Wu, C.; Jin, Z.; Xu, L. *Sci. Seric.* **1993**, *19*, 105.
31. Magoshi, J. *Kobunshi Ronbunshu* **1974**, *31*, 463.
32. Tsukada, M.; Gotoh, Y.; Nagura, M.; Minoura, N.; Kasai, N.; Freddi, G. *J. Polym. Sci. Part B: Polym. Phys.* **1994**, *32*, 961.
33. Um, I.; Kweon, H.; Park, Y.; Hudson, S. *Int. J. Biol. Macromol.* **2001**, *29*, 91.
34. Viles, J.; Cohen, F.; Prusiner, S.; Goodin, D.; Wright, P.; Dyson, H. *Proc. Natl. Acad. Sci. U. S. A.* **1999**, *96*, 2042.
35. Chen, X.; Li, W.; Yu, T. *J. Polym. Sci. Part B: Polym. Phys.* **1997**, *35*, 2293.
36. Xie, X.; Zhou, P.; Deng, F.; Wu, P.; Zong, X.; Yao, W. *Chem. J. Chin. Univ. Chin.* **2004**, *25*, 961.
37. Chen, X.; Shao, Z.; Marinkovic, N.; Miller, L.; Zhou, P.; Chance, M. *Biophys. Chem.* **2001**, *89*, 25.
38. Nam, J.; Park, Y. *J. Appl. Polym. Sci.* **2001**, *81*, 3008.
39. Lawrence, B.; Marchant, J.; Pindrus, M.; Omenetto, F.; Kaplan, D. *Biomaterials* **2009**, *30*, 1299.
40. Gil, E.; Mandal, B.; Park, S.; Marchant, J.; Omenetto, F.; Kaplan, D. *Biomaterials* **2010**, *31*, 8953.